sciendo
Polish Journal of Medical Physics and Engineering
The Journal of Polish Society of Medical Physics
ISSN 1898-0309, doi: 10.2478/pjmpe-2019-0013
June 2019
Vol 25, Issue 2

Scientific Paper

A GATE Monte Carlo model for a newly developed small animal PET scanner: the IRI-microPET

S.Z. ISLAMI RAD[1,a], R. Gholipour PEYVANDI[2,b], M.K. SADEGHI[2,c]

[1]*Department of Physics, Faculty of Science, University of Qom, Ghadir Blvd, P. O. B. 3716146611, Qom, Iran*

[2]*Faculty of Physics, Shahrood University of Technology, Shahrood, Iran*

[a]*E-mail address: szislami@qom.ac.ir*

[b]*E-mail address: rgholipour@shahroodut.ac.ir*

[c]*E-mail address: mohammadkazem.sadeghi@yahoo.com*

(received 24 April 2018; revised 18 December 2018 and 19 February 2019; accepted 26 March 2019)

Abstract

Monte Carlo simulation is widely used in emission tomography, in order to assess image reconstruction algorithms and correction techniques, for system optimization, and study the parameters affecting the system performance. In the current study, the performance of the IRI-microPET system was simulated using the GATE Monte Carlo code and a number of performance parameters, including spatial resolution, scatter fraction, sensitivity, RMS contrast, and signal-to-noise ratio, evaluated and compared to the corresponding measured values. The results showed an excellent agreement between simulated and measured data: The experimental and simulated spatial resolutions (radial) for ^{18}F in the center of the AFOV were 1.81 mm and 1.65 mm, respectively. The difference between the experimental and simulated sensitivities of the system was <7%. Simulated and experimental scatter fractions differed less than 9% for the mouse phantom in different timing windows. The validation study of the image quality indicated a good agreement in RMS contrast and signal-to-noise ratio. Also, system performance was compared with the two available commercial scanners which were simulated using GATE code. In conclusion, the assessment of the Monte Carlo modeling of the IRI-microPET system reveals that the GATE code is a flexible and accurate tool for describing the response of an animal PET system.

Key words: GATE; Monte Carlo; simulation; IRI-microPET; performance.

Introduction

Monte Carlo simulations are extensively used in imaging systems including single-photon emission tomography (SPECT) and positron emission tomography (PET), in order to study the effect of different parameters on system performance under various conditions, evaluate the performance of algorithms for image reconstruction, scatter correction, and protocol optimization. Several validation studies of GATE (Geant 4 Application for Tomographic Emission) for the modeling of different small-animal PET systems were done and the physical characteristics and performance of such systems were discussed. The evaluated animal PET systems were Mosaic, OPET, GE Advance/Discovery LS, Philips Allegro/GEMINI, Focus 120 and Inveon [1-6].

In this research, GATE (Geant 4 Application for Tomographic Emission-version 5.0.0) was presented as a Monte Carlo simulation toolkit for simulating and validation an animal positron emission tomography system (IRI-microPET). In order to optimize image quality and overall performance, this system had been built and tested at the Nuclear Science and Technology Research Institute (NSTRI- Gamma scan Laboratory) [7].

Also, in order to validate our model, the simulation data was acquired in ASCII format. Images were reconstructed with the implementation of the MLEM algorithm on acquired ASCII sinogram data by using an in-house program written in MATLAB (R2015a).

Next, prior to the application of the system to actual biological studies, NEMA performance parameters including spatial resolution, scatter fraction, and sensitivity, as well as image quality, were evaluated and compared to the corresponding experimentally measured results. For validation, simulated results were compared to available performance measurements for other small-animal PET systems.

Materials and methods

IRI-microPET: system description

The IRI-microPET (Islamic Republic of Iran) was constructed and designed at the NSTRI [7]. The scanner consists of four detectors so that each detector was positioned at a distance of

50 mm from the axis of rotation on a rotating gantry. Each detector was composed of 2×2 cm^2 of pixelated LYSO (Lutetium Yttrium Oxyorthosilicate) matrix of 10×10 crystals (2×2 mm^2 wide and 10 mm deep) (**Figure 1**). Each block LYSO pixelated detector was coupled to a PS-PMT (Position Sensitive Photomultipliers Tube). The PS-PMT (R8900U-00-C12) consists of 6X anode plates plus 6Y anode plates that collect the amplified charges produced by the crystal. The Fast-slow preamplification was used in our constructed animal PET[8]. The slow circuits were used to determine the radiation position by integrating the anode outputs. In order to characterize the event, a photon pair which triggers the energy and position signals should be detected. An Anger-type logic DPC (Discretized Positioning Circuit) resistive chain reduced the output signals from the crystal-PS-PMT modules to 4. The X and Y positions were fed into the shaping amplifier. The amplified last dynode signals of PS-PMT in fast preamplifier were sent to constant fraction discriminator (CFD. Different energy windows with lower and upper energy levels; 300–700 keV, 400–700 keV, 400–600 keV, 300–600 keV, 350–700 keV and 350–650 keV were selected in this section for image reconstruction. For detecting the coincidence events, the timing signals were sent to coincidence module with a coincidence window of 4 ns and 2.4 ns timing resolution. Then, the data were sent to Gate and Delay. Finally, the data were collected and analyzed using data acquisition PD-MFS-2MS/s-8/14 board for determining the energy and position of pair gamma photons. The board was controlled using a computer. The processing and reconstructing of the resulting data were performed with this computer.

Simulation software

In accordance with the user guide Gate [9], a typical GATE simulation consists of following modules.

Geometry

The scanner and phantoms were modeled as simple shapes in accordance with the IRI-microPET scanner (the real system). The most relevant system parameters of IRI-microPET was summarized in **Table 1**. The tolerances and dimension of phantoms based on the NEMA-like standard (NEMA NU-4-2008) should be considered in modeling using GATE code.

Table 1. IRI-micro PET system parameters.

Parameter	IRI-micro PET
Crystal material	LYSO
Crystal size	2.0×2.0×10 mm^3
Crystal pitch	0.675 mm
Crystal array	100 (10×10)
Number of detectors	4
Number of crystals	400
Axial FOV	20 mm
Transverse FOV	20 mm
Radial FOV	50 mm (ring diameter)

Digitizer

The digitizer in GATE can convert photon interactions into counts according to real scanner's detectors and electronics. Some functions were categorized in the digitizer to simulate the detection parameters which each of them was represented by a module. The crystal blurring, crystal quantum efficiency (QE), thresholder, upholder, dead time and other electronics delay were defined in this section. The digitizer has a sequence in signal processing. At first, the Adder module collected the deposited energy of a particle within a crystal. The acquired data from the Adder module within a block of crystals were integrated using the readout module to create a pulse. Next, a detection efficiency factor and an energy resolution of 25% referenced at 511 keV to the collected interactions within the detector blocks were applied using a Blurring module. An energy-window discriminator (CFD module in a real system) was then applied via the thresholder and upholder modules either 300 to 700 keV. Also, a 150 ns non-paralyzable dead time for the delayed and prompt events was used to simulate lost data by the written program by our group. At last, the resulting pulses were sorted using the coincidence module with 4 ns timing window [9].

Physics

All interactions and processes from source decay to the photons detection were simulated using the GATE code [9].

Source

The source geometry, particle type, activity, half-life, emission angle, and source movement were defined in this section. It is important to note that the geometry, activity and source type are dependent on the particular experimental design to describe the response of the simulated animal PET system.

Data Output

Different output formats are available for different imaging, such as ASCII, ROOT, Interfile, LMF, and ECAT which ASCII output was used for our purpose. Images were reconstructed with the implementation of the MLEM algorithm on acquired ASCII sinogram data by using an in-house program written in MATLAB (R2015a).

Finally, the code was validated via comparison with measured data for NEMA measurements of the IRI-micro PET scanner published by Islami rad et al. [7,9].

MLEM algorithm

The produced sinograms from ASCII data were reconstructed using Maximum likelihood expectation maximization (MLEM) algorithm. This statistic reconstruction method is based on data Poisson characteristic which it tries to maximize the log-likelihood in each iteration step. In this research, 40 iterations were used for image reconstruction.

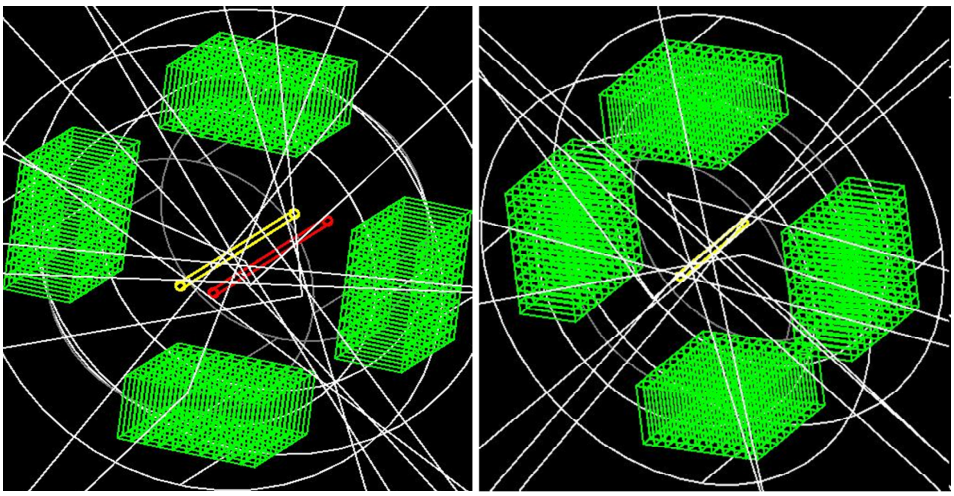

Figure 1. Geometry and position of the simulated phantom for spatial resolution measurement.

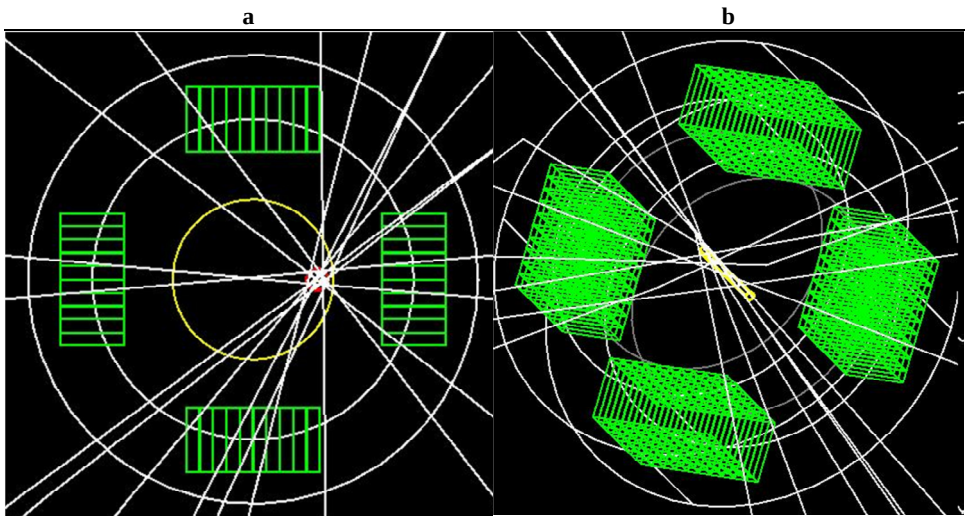

Figure 2. The position of the NEMA phantom within the simulated scanner geometry for (a) the scatter fraction and (b) sensitivity performance assessment.

Performance evaluation

The assessment of system performance in terms of NEMA parameters such as spatial resolution, scatter fraction, sensitivity and image quality was carried out as an important precondition before the simulated data was replaced with real data for a reliable description of the system response function. Thus, these parameters were simulated according to the NEMA-like standard.

Spatial resolution

Spatial resolution was calculated by measuring the width of the profile obtained. According to the reported researches and NEMA characteristics, the resolution should be determined using the ^{22}Na point source with a dimension of less than 0.3 mm in diameter. The fabricating of actual sources with such small dimensions was difficult for our group. Thus, more practical line sources were modeled. The simulated glass capillaries with an inner diameter of 1.15 mm and the outer diameter of 1.55-mm were filled with ^{18}F radioactive materials (2.2 MBq activity). The resolution quantities were measured at the central slice of the FOV, at a radial distance of 5 mm from the geometric center of the imaging gantry. These measurements were also taken at the same transaxial points at ¼ axial FOV (**Figure 1**). The acquired data at 0 mm position was not included in the NEMA protocol, although the data at this position were measured. The MLEM algorithm was used to reconstruct the acquired sinograms. Then, the spatial resolution was measured as the FWHM of the profiles (Full Width at Half-Maximum) in the radial directions [7,10,11]. These measurements were performed in real condition.

Scatter fraction

Scatter fraction is an important parameter for comparing the efficiency of PET scanners. IRI-microPET was constructed for imaging small animals such as mice. Thus, the mouse phantom was modeled for determining the scatter fraction. According to the proposed geometry of NEMA NU 4-2008, a polyethylene phantom with cylindrical geometry and 0.9670.1 g/cm^3 density

was simulated with a diameter 25 ± 0.5 mm and length of 70 ± 0.5 mm. A hole with cylindrical geometry and a diameter of 3.2 mm was drilled parallel to the central axis at a radial distance of 10 mm and the line source (filled with ^{22}Na) was placed in the hole. The mouse phantom was located at the center of the system and the scanning process was performed for different energy windows (**Figure 2a**). Also, scatter fraction calculation was performed for simulated and real data with different timing windows (4 ns, 8 ns, 10 ns, 16 ns, and 20 ns) [11,12].

Sensitivity

According to the real condition, a ^{22}Na source with an inner diameter of 1 mm and 1 µCi activity as a point source was located at the center of the axial field of view (AFOV) of the simulated IRI-microPET scanner (**Figure 2b**). Different energy windows with lower and upper energy levels such as 300–700 keV, 400–700 keV, 400–600 keV, 300–600 keV, 350–700 keV and 350–650 keV were regulated in GATE simulation together with a fixed coincidence timing window of 4 ns in order to determine the sensitivity parameter. The count rates of prompt and random coincidence were calculated and the true coincidence count rates were measured by subtracting the random count rates from the prompt count rates. The sensitivity was defined as the rate of the true coincidence counts to the source activity (1 µCi) [13].

Image quality

In order to investigate the image quality of our animal PET, a cylindrical phantom with 3 mm inner diameter as a vial (filled with ^{22}Na) was scanned. The coronal and axial slices of the phantom were reconstructed using the MLEM algorithm [14]. Finally, the quality of images was evaluated by RMS contrast and SNR factors [15,16].

RMS contrast

One of the most important factors in demonstrating image quality is RMS contrast. The contrast is a characteristic which represents the diversity of in visual properties that make an object distinguishable from other objects and the background. In order to compare the image qualities, RMS contrast was selected. RMS contrast was explained as the standard deviation of the pixel intensities.

$$\mathrm{RMS\,contrast}=\sqrt{\frac{1}{MN}\sum_{i=0}^{N-1}\sum_{j=0}^{M-1}(I_{ij}-\bar{I})^2} \qquad \text{Eq. 1}$$

where intensities I_{ij} was the i-th and j-th elements of the two-dimensional image of size M by N. The average intensity for all pixel values in the reconstructed image was defined as $\bar{I}$. In order to have the range of intensity values between 0 and 1, I or image pixels should be normalized. Thus, the reconstructed images in each energy window were normalized to intensity range with the highest value. This process was performed to compare all of the reconstructed images [17,18].

Signal to noise (SNR)

The signal to noise parameter is defined as the ratio the signal value to the noise quantity. The signal for a reconstructed image was computed as the difference between the mean activity in an interest region and a background region and the noise was determined as the standard deviation of pixel values for background region [18].

Results

Spatial resolution

The spatial resolutions (FWHM) as radial and tangential at the center of the FOV were measured 1.65 mm and 1.73 mm, respectively. Also, the FWHM values were determined 1.80 and 1.90 mm at a radial offset of 5 mm. These measurements were performed for the same transaxial points at axial FOV, and insignificant differences were observed from the acquired data (**Table 2**). **Figure 3** displayed the acquired sinogram and reconstructed images by MLEM algorithm for spatial resolution calculation using GATE. Also, the results measured by IRI-microPET were shown in **Table 2**. According to the results, the spatial resolution for acquired images from the GATE is less than the real data. The simulated results were better than measured values because we could not simulate some processes such as light sharing between PMTs and light spreading.

Scatter fraction

The scatter fraction parameter were measured for mouse-sized phantom (^{22}Na line source inside the phantom) and different energy windows (**Table 3**). The comparison of scatter fraction quantities for different energy and timing windows were shown in **Figure 4**. According to results, the scatter fraction decreased with reducing timing window and the width of the energy window. The simulated data with GATE code were compared with the measured data (IRI-microPET). The presented scatter fractions are very close to the measured data within 5% to 9%.

Sensitivity

A comparison was performed between the simulated and measured [7] sensitivity for different energy windows with a timing window of 4 ns (**Table 4** and **Figure 5**). A good agreement was observed between simulations and measurements with a maximum difference of less than 7%.

Image quality

The reconstructed images using the measured and simulated results were shown in **Figure 6**. Image quality was assessed by RMS contrast and SNR factors whose results were obtained in **Table 5**. As expected from the results, a good agreement was observed between simulated and measured results. An average absolute difference of 10% was observed between simulated and measured RMS contrast values. Also, SNR for the images reconstructed using the simulation datasets was better than the measured data (but the difference is less than 9.6%).

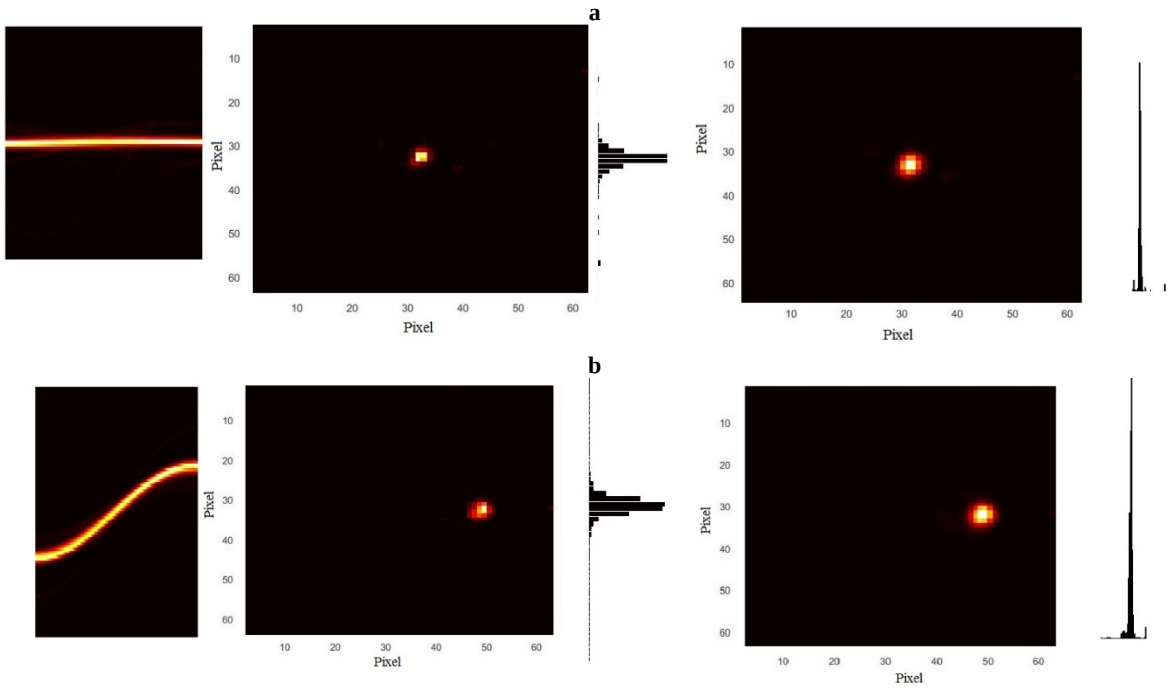

Figure 3. The radial (left) and tangential (right) spatial resolution for a point source (a) at the center of FOV and a (b) radial offset of 5 mm (at the center of the AFOV).

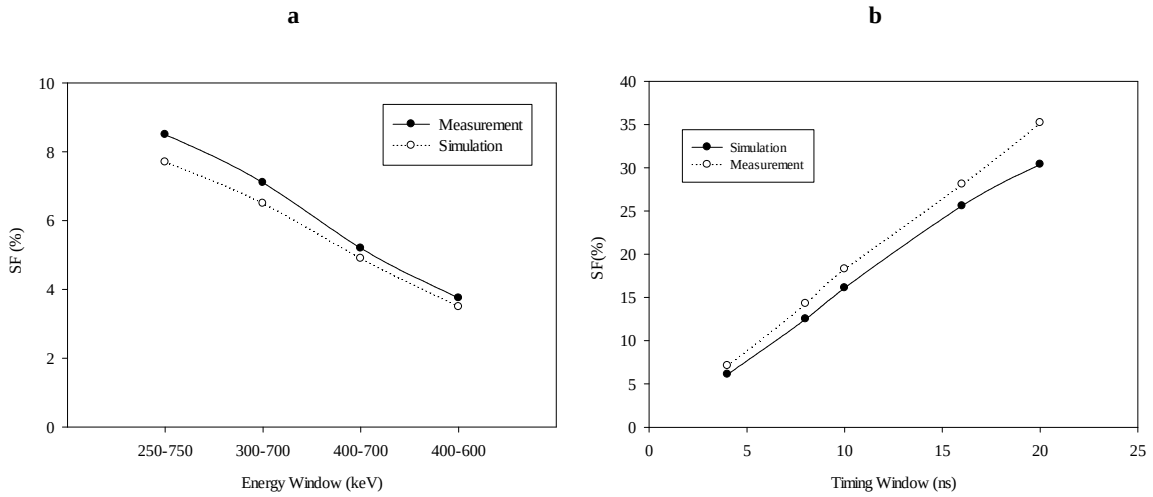

Figure 4. Measured and simulated scatter fraction values for (a) different energy windows (b) different timing windows.in IRI-microPET.

Table 2. Spatial resolution results for different axial, radial and tangential positions, for both measured and simulated point sources at corresponding locations within the FOV.

Radial offset (mm)	Tangential FWHM (mm)		Radial FWHM (mm)	
	measurement	simulation	measurement	simulation
		at axial center		
0	1.90	1.73	1.81	1.65
5	2.06	1.90	1.96	1.80
		at ¼ axial FOV		
0	1.88	1.78	1.92	1.76
5	1.98	1.88	2.03	1.81

Table 3. Simulated scatter fraction (SF) values for the IRI-micro PET scanner compared with measurements.

Energy window (keV)	Measured SF (%)	Simulated SF (%)
250-750	8.5	7.7
300-700	7.1	6.5
400-700	5.2	4.9
400-600	3.75	3.5

Table 4. Measured and simulated sensitivity of the IRI-micro PET system for different energy window widths.

	Lower energy threshold (keV)	Upper energy threshold (keV)		
		600	650	700
Measurement	300	1.61	1.70	1.74
	350	1.51	1.55	1.58
	400	1.24	1.29	1.35
Simulation	300	1.70	1.79	1.84
	350	1.58	1.59	1.67
	400	1.34	1.35	1.46

Figure 5. Comparison of the simulated and measured sensitivity for different energy windows with 4 ns timing window.

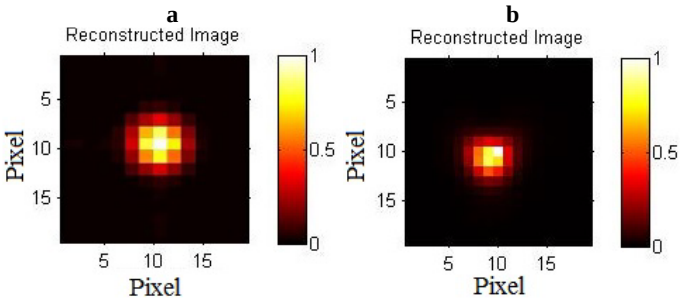

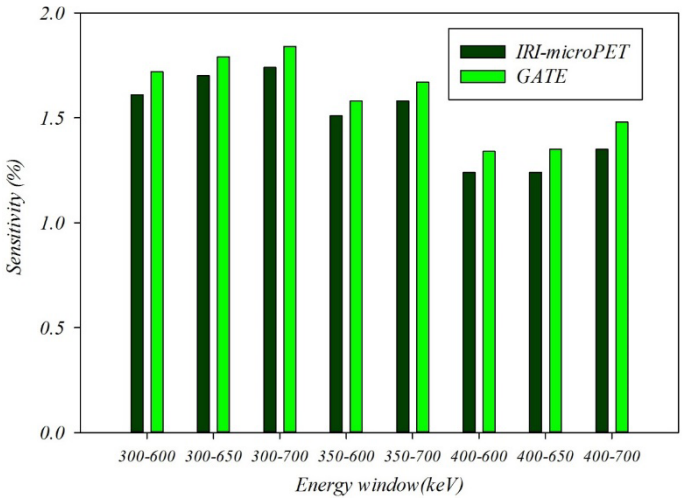

Figure 6. The reconstructed images by MLEM algorithm using (a) simulation and (b) experimental data.

Table 5. RMS contrast and SNR quantities (measurement and simulation) of reconstructed images by MLEM algorithm.

	Simulation	Measurement
RMS contrast	0.099560	0.11094
SNR	7.98	7.21

Discussion

The purpose of this work was to develop a Monte Carlo model of the IRI-microPET scanner based on GATE code. Then, its accuracy was evaluated in comparison with the IRI-microPET data and the other simulated micro-PET scanners data. The validation of our model was based on some NEMA-like (NEMA NU-4 2008) standards protocols for the evaluation of PET scanners' performance which was composed of spatial resolution, scatter fraction and sensitivity. Finally, the performance at the image level was assessed using an image quality phantom based RMS contrast and SNR.

The acquired spatial resolutions with GATE simulation were better than the measurements. The difference between simulated and experimental data was due to the inability to simulate the detection processes such as light sharing between PMTs. In the case of the IRI-microPET, the differences were between 5 and 11%.

The scatter fractions for different energy and timing windows were measured as simulation and experimental which the results observed a good accuracy in produced data from IRI-microPET models. The variation between the acquired data from the simulation and experimental was a minimum of 5% to a maximum of 9%.

Also, the accuracy differences were less than 7% between the simulated and the measured sensitivity.

The same algorithm was used for image reconstruction and correction of the measured and simulated dataset. Thus, there is an unbiased and accurate assessment of simulated image quality. A good agreement between simulated and measured RMS contrast was established for cylindrical phantom (3 mm diameter). Also, the close agreement on signal-to-noise ratio indicated that the accuracy of our developed model was sufficient and reasonable.

In addition, for achiving the validation of our model, the simulated data were compared with simulated data animal PET scanners (Inveon and Focus 120) [6]. The evaluation was performed according to the approved NEMA NU-4 2008 recommendations in order to facilitate the comparison between small-animal PET scanners. This comparison was inaccurate due to some differences in source geometries, materials, and methods. The comparison between IRI-microPET parameter (simulated and measured) and those for Inveon and Focus was represented in **Table 6**.

The experimental and simulated sensitivity for a point source in the center of FOV and an energy window of 350–650 keV was calculated 1.55% and 1.59%, respectively. The produced results were lower than those obtained for Focus 120 and Inveon. It was important to note that IRI-microPET was a four-block scanner, the main reason that reduced its sensitivity.

Table 6. Comparison between various IRI-microPET parameters (simulated and measured) and those for Inveon and Focus 120.

Parameter	IRI-microPET		Inveon	Focus 120
	measured	simulated		
Scatter fraction[a]	Mouse phantom (Ø=25 mm, *L*= 70 mm)	Mouse phantom (Ø=25 mm, *L*= 70 mm)	Mouse phantom (Ø=25 mm, *L*= 70 mm)	Mouse phantom (Ø=30 mm, *L*= 70 mm)
	8.5	7.7	19.2	18.9
Sensitivity (%)	350-650 keV, 4 ns	350-650 keV, 4 ns	350-650 keV, 6 ns	350-650 keV, 6 ns
	1.55	1.59	8.00	5.00

According to NEMA protocol, a mouse phantom was used to calculate the scatter fraction. Based on comparison with the results reported in researches, the scatter fraction of our scanner (simulated and measured) was less than that of Inveon and Focus 120.

The comparison and simultaneous assessment of spatial resolution, RMS contrast, and SNR parameters only were considered in this study. Thus, we cannot compare these parameters with other animal PET scanner.

Conclusion

In this paper, a comparison was performed between the acquired simulated and measured data by the IRI-micro PET system. Also, these results were compared with some simulated microPET scanners. The results of this research indicate that GATE can accurately simulate the main performance characteristics of the IRI-micro PET scanner. Some parameters including spatial resolution, scatter fraction, sensitivity, RMS contrast, and SNR can be accurately simulated using GATE's digitizer and NEMA-like protocols. The validation of our model can be useful in data correction algorithms, the optimization of emission acquisition protocols and validation of reconstruction. We only used the ASCII data for image formation in this study which acquired results can be valuable for all of the medical imaging systems such as PET and SPECT. In the next researches, the acquired information from GATE simulations will use in the future improvement of image quality and performance of PET scanner.

References

[1] Merheb C, Petegnief Y, Talbot N. Full modeling of the MOSAIC animal PET system based on the GATE Monte Carlo simulation code. Phys Med Biol. 2007;52(3):563-576.

[2] Merheb C, Nicol S, Petegnief Y et al. Assessment of the Mosaic animal PET system response using list-mode data for validation of Gate Mote Carlo modeling. Nucl Inst Meth A. 2006;569(2):220-224.

[3] Rannou FR, Kohli V, Prout DL, et al. Investigation of OPET performance using GATE, a Geant4-based simulation software. IEEE Trans Nucl Sci. 2004;51(5):2713-2717.

[4] Schmidtlein CR, Kirov AS, Nehmeh SA, et al. Validation of GATE Monte Carlo simulation of the GE Advance/Discovery LS PET scanners. Med Phys. 2006;33(1):198-208.

[5] Lamare F, Turzo A, Bizais Y et al. Validation of a Monte Carlo simulation of the Philips Allegro/GEMINI PET systems using Gate. Phys Med Biol. 2006;51(4):943-962.

[6] Kim JS, Lee JS, Park MJ, et al. Comparative Evaluation of Three MicroPET Series Systems Using Mont Carlo Simulation: Sensitivity and Scatter Fraction. IEEE Nucl Sci Sym Conf. 2007;4534-4535.

[7] Islami rad SZ, Gholipour Peyvandi R, Askari lehdarboni M, Ghafari AA. Design and performance evaluation of a high resolution IRI-microPET preclinical scanner. Nucl Instr and Meth A. 2015;781:6-13.

[8] Islami rad SZ, Shamsaei Zafarghandi M, Gholipour Peyvandi R et al. Study of the Slow-Fast preamplifier input parameters effects on output image for LYSO scintillator with PS-PMT based animal PET. Instr & Exp Tech. 2014;57(4):488-493.

[9] GEANT4 Collaboration, GEANT4: A simulation toolkit, Jun (2009).

[10] Canadas M, Embid M, Lage E, et al. NEMA NU 4-2008 performance measurements of two commercial small animal PET scanners: Clear PET and rPET-1. IEEE Trans Nucl Sci. 2011;58(1):58-65.

[11] Yang Y, Tai Y, Siegel C, et al. Optimization and performance evaluation of the microPET II scanner for in vivo small-animal imaging. Phys Med Biol. 2004;49(12):2527-2545.

[12] Motta A, Damiani C, Del Guerra A, et al. Use of a fast EM algorithm for 3D image reconstruction with the YAP-PET tomograph. Comput Med Imaging Graph. 2002;26(5):293-302.

[13] Constantinescu CC, Mukherjee J. Performance evaluation of an Inveon PET preclinical scanner. Phys Med Biol. 2009;54(9):2885-2899.

[14] Fahey FH. Data Acquisition in PET Imaging. J Nucl Med Technol. 2002;30(2):39-49.

[15] Jiang M, Wang G. Convergence of the simultaneous algebraic reconstruction technique (SART). IEEE Trans Imag Process. 2003;12(8): 957-961.

[16] Herman GT. Fundamentals of Computerized Tomography: Image Reconstruction from Projections. Springer (2009).

[17] Gholipour Peyvandi R, Islami rad SZ, Heshmati R, et al. Influence of projection steps on image quality using single source–single detector gamma ray tomograph. Instr and Exp Tech. 2011;54(4):542-547.

[18] Lodge MA, Rahmim A, Wahl RL. Simultaneous measurement of noise and spatial resolution in PET phantom images. Phys Med Biol. 2010;55(4):1069-1081.